



OPEN **Discussing the epidemiology of COVID-19 model with the effective numerical scheme**

Abeer Aljohani¹, Shahbaz Mustafa², Shan Ali Khan³, Abdullah Alhushaybari⁴ & Herbert Mukalazi⁵✉

COVID-19 is a contagion that's container lead to lung difficulties such as pneumonia and, in the greatest severe circumstances, serious respirational disease. In response to these challenges, the present research proposes and analyses an SEIQR model with a nonlinear recovery and incidence rate. The appearance aimed at fundamental threshold quantity (\mathcal{R}_0) is established, which is critical to the stability of disease-free and endemic equilibria. A non-standard Finite difference (NSFD) Scheme is developed and for the model, and the denominator function is select so that the proposed structure maintains solution boundedness. It is demonstrated that the NSFD scheme is not dependent on the step size produces superior outcomes in totally admirations. The Jacobian approach is employed to establish the local stability of the disease free equilibrium, while Schur-Cohn conditions are used for the endemic equilibrium point in the the discrete NSFD scheme. The Enastu Criterion and the Lyapunov Function are used to demonstrate the global stability of the disease free and endemic equilibria. Numerical simulation are also presented to discuss the benefits of the NSFD scheme and to validate the theoretical conclusions. Calculated simulations show that the NSFD method preserves the important aspects of the continuous model. As a result, they generate estimates that align consistently with the model's solutions.

Keywords Incidence rate, Local and global stability, Lyapunov function, Numerical simulations

By the end of 2019, Wuhan, China, was the source of the corona virus 2019 (COVID-19), which is caused by SARS-COV-2 (severe acute respiratory syndrome corona virus 2). Subsequently, the epidemic\pandemic swiftly spread reached over 210 nations^{1,2} and continues to pose serious health and socioeconomic difficulties in several regions of the globe. Scientists continue to develop safe COVID-19 vaccines and advance innovative diagnostics. As of now, there isn't a safe and efficient vaccination or antiviral to combat the pandemic. International and local communities are focused on identify key parameters that influence the virus transmission to control its spread. Various government estimates suggest various preventive strategies to stop the spread of COVID-19, such as wearing a mask, maintain a physical distance, routinely weekly wash your fingers, and escaping sickening persons^{3,4}.

The infectious disease COVID-19 can be transmitted by direct human contact as well as droplet aerosols⁵⁻⁷. This illness has ruined many people with few resources across various countries, making it a serious problem for human society. Since COVID-19 is more contagious and more likely to cause a pandemic than SARS, it has spread quickly over the world. This World health Organization (WHO) declared the COVID-19 flare-up to be a global pandemic on March 11 due to the significant increase in the spread of the infection. Fever, cough, malignancy, exhaustion, sputum production, headache, diarrhoea, dyspnoea, and lymphopenia are the signs and symptoms of COVID-19⁸. COVID-19 can result in pneumonia and possibly mortality in more severe situations¹. COVID-19 can take up to 14 days to incubate, with a median of about 5.2 days⁹. A useful tool to concentrate on the mechanism via that a viral illness can spread over a population is mathematical modelling.

Evaluating the safety and quality of vaccinations is the primary goal of the World Health Organization (WHO). In order to ensure vaccine efficacy, WHO works together with researchers throughout the globe to create and implement international standards and norms. While some scientists have researched models of dynamic delaying differential for the COVID-19 outbreak^{10,11}, many others have been drawn to develop alternative models¹²⁻¹⁶ that deal with vaccination strategies to limit the spread of epidemic diseases. Recently, a

¹Department of Computer Science, Applied College, Taibah University, Medina 42353, Saudi Arabia. ²Department of Mathematics, Institute of Numerical Sciences, Gomal University, Dera Ismail Khan 29050, KPK, Pakistan. ³School of Energy and Power Engineering, Xian Jiaotong University, Xi'an 710049, China. ⁴Department of Mathematics, Turabah University College, Taif University, Taif, Saudi Arabia. ⁵Department of Mathematics and Statistics, Faculty of Basic Science, Kyambogo University, Kampala, Uganda. ✉email: hmukalazi@kyu.ac.ug

number of articles^{17–22} on the effectiveness of newly approved vaccinations have been released. To the best of our knowledge, a few research studies^{17,23} have been released in an effort to shed light on the relationship between vaccine choice and the (COVID-19) epidemic's expansion. No one has ever fully analysed the Corona pandemic mathematically using a vaccination model.

The differential equations utilised in the models that were given had some restrictions on their order, but they were still based on classical derivatives. Butt et al. provide a description of the mathematical model of Corona illness in²⁴. Using the integer order SEIQR epidemic model, the author examined the corona virus disease. This study determines the fundamental reproduction number in addition to containing the discrete model, finding the fundamental reproduction number in order to assess stability.

The current paper is organized in a friendly manner. In “Derivation of corona model” section, the mathematical model is introduced and its parameters are thoroughly examined also describe the flow chart of Fig. 1. The fundamental reproduction numbers are defined and analyzed in “Flow diagram” section. The global stability of the disease-free conditions under the NSFD scheme is assessed using the properties of the Lyapunov function in “Feasible region of corona model” section, which also discusses the local stability of the disease-free equilibrium point using the Schur-Cohn criterion. We agree that the numerical solution of the system of ODEs contributes to the methods' comparatively large complexity. The results are given in the closing segment to represent the entire manuscript.

Derivation of corona model

Depending on how the corona virus disease spreads, a number of alternative mathematical models with varying assumptions have been proposed in the literature to far^{25,26}. These models offer numerous benefits to public health planners and policy makers. By adding a class of vaccinated humans, we have created a new SEIQR COVID-19 pandemic model for the actual world in this part.

The following variables were used to model the dynamics of the coronavirus's transmission among individuals: The human population at time t is divided into five divisions by the model in the susceptible $S(t)$, exposed $E(t)$, infected $I(t)$, quarantine $Q(t)$ and recovered $R(t)$. are the entities in question.

The following set of ordinary differential equations, which are taken from Fig. 1, describe the SEIQR mathematical framework for the corona virus circulation in an organization:

Flow diagram

$$\begin{aligned}
 \frac{dS}{dt} &= \rho - \tau_1 S I - \tau_2 S E - \omega S \\
 \frac{dE}{dt} &= \tau_1 S I + \tau_2 S E - (v_1 + \omega + \Lambda + \varphi) E \\
 \frac{dI}{dt} &= \Lambda E - (\omega + \theta_1 + c) I \\
 \frac{dQ}{dt} &= v_1 E - (\delta + \omega + \theta_2) Q \\
 \frac{dR}{dt} &= \varphi E + c I + \delta Q - \omega R.
 \end{aligned}
 \tag{1}$$

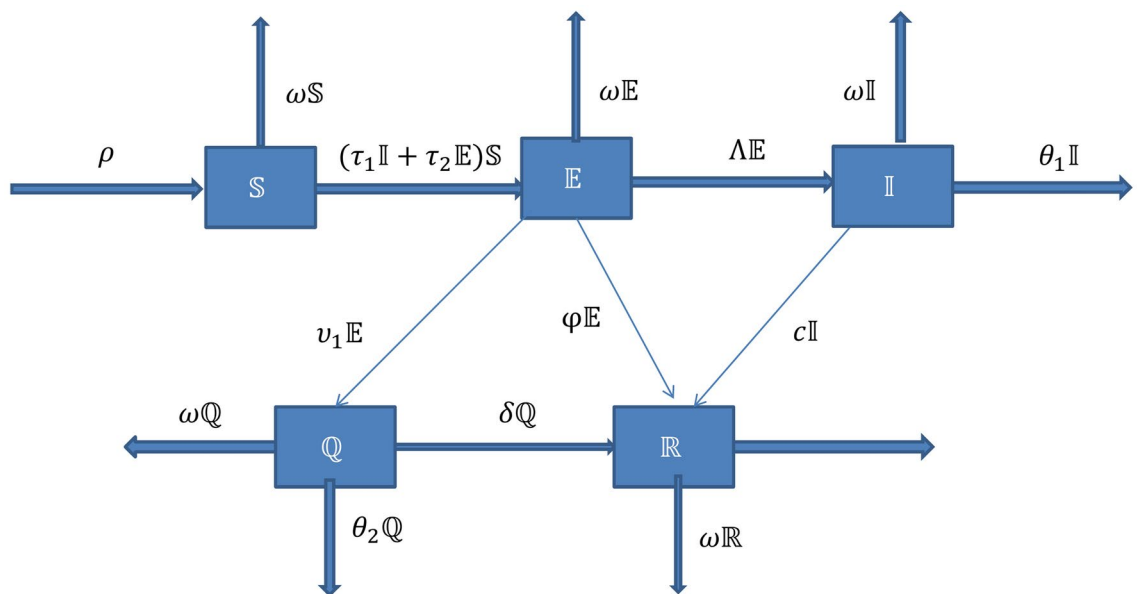


Fig. 1. A graphic depiction of the illness energetic in a compartmental model (1).

With $S(0) > 0, E(0) > 0, I(0) > 0, Q(0) > 0$ and $R(0) > 0$.

The state variable and related limits of the recently proposed paradigm, known as COVID-19 are explained in depth in model (1).

Feasible region of corona model

Adding above five equations of the system (1), we have

$$N(t) = S + E + I + Q + R$$

$$\frac{dN}{dt} = \rho - \omega S - v_1 E - \omega E - \omega I - \theta_1 I + p_1 E - \omega Q - \theta_2 Q - \omega R$$

From above eq. we can write

$$\frac{dN}{dt} \leq \rho - \omega S$$

And

$$\lim_{n \rightarrow \infty} SUP N \leq \frac{\rho}{\omega}$$

where $N(t)$ is the original inhabitants scope. In specific, $N(t) \geq \frac{\rho}{\omega}$. Thus N and entirely extra variable of the ideal (1) are circumscribed in a section. Thus

$$\Pi = \left\{ (S, E, I, Q, R \in \mathbb{R}_+^5; 0 \leq N(t) \leq \frac{\rho}{\omega} : S, E, I, Q, R \geq 0) \right\}. \tag{2}$$

Equilibrium point

A unique non- negative Corona free equilibrium for the model (1) Exist at the point.

- a. Disease Free Equilibrium (DFE) = $(\frac{\rho}{\omega}, 0, 0, 0, 0)$
- b. Disease Endemic Equilibrium (DEE) = $(S_a^*, E_a^*, I_a^*, Q_a^*, R_a^*)$

$$S_a^* = \frac{(v_1 + \varphi + \Lambda + \omega)(c + \omega + \theta_1)}{\tau_1 \Lambda + \tau_2 (c + \omega + \theta_1)} > 0,$$

$$E_a^* = \frac{(\rho - \omega S_a^*)(c + \omega + \theta_1)}{\tau_1 \Lambda + \tau_2 (c + \omega + \theta_1) S_a^*} > 0,$$

$$I_a^* = \frac{\Lambda E_a^*}{(c + \omega + \theta_1)} > 0,$$

$$Q_a^* = \frac{v_1 E_a^*}{(\rho + \omega + \theta_2)} > 0,$$

$$R_a^* = \frac{1}{\omega} [\varphi E_a^* + c I_a^* + \delta Q_a^*] > 0.$$

Threshold quantity (\mathcal{R}_0)

An estimate derived from epidemiological foundations, the basic reproduction ratio shows the total number of related diseases that result from a only diseased soul in a society that is entirely exposed to the illness throughout that time. The matrices developed for the original disease and the prerequisite for the illness evolution are F(x) and M(x). We used the same methodology as defined in²⁷.

Suppose

$$\mathcal{F}(x) = \begin{pmatrix} \tau_1 S I - \tau_2 S E \\ 0 \\ 0 \\ 0 \\ 0 \end{pmatrix}.$$

And

$$\mathcal{M}(x) = \begin{pmatrix} (v_1 + \omega + \Lambda + \varphi) E \\ (\omega + \theta_1 + c) I - \Lambda E \\ (\delta + \omega + \theta_2) Q - v_1 E \\ \omega S - \rho \\ \omega R - \varphi E - c I - \delta Q \end{pmatrix}.$$

The amount of transmission into and available of the exposed, infected, and quarantine classes, as well as the rate of original contagion positions entering, are represented by functions F and M, accordingly, as fellows

$$F = \begin{pmatrix} \tau_1 S I - \tau_2 S E \\ 0 \\ 0 \end{pmatrix},$$

where the transition rate of a present or moved case is represented by matrix M , which is calculated as

$$M = \begin{pmatrix} (v_1 + \omega + \Lambda + \varphi) E \\ (\omega + \theta_1 + c) I - \Lambda E \\ (\delta + \omega + \theta_2) Q - v_1 E \end{pmatrix}.$$

The number of \mathcal{R}_0 for the model (1) is the largest absolute eigenvalue of the matrix gives the basic reproduction number, \mathcal{R}_0 . In terms of terminology,

$$\mathcal{R}_0 = \frac{\rho[\tau_1 \Lambda + \tau_2(c + \omega + \theta_1)]}{(c + \omega + \theta_1)(v_1 + \varphi + \Lambda + \omega)}.$$

Non-standard finite difference scheme (NSFD)

We propose an NSFD approach for model (1). The plan is based on the non-standard finite difference numerical modelling known as Mickens Theory^{28–31}. Specify the kinds of problem solved using NSFD scheme or rephrase for precision^{29,32}. In these cases, it is essentially necessary that the mathematical answer achieved preserves each property of a dynamic model. It is demonstrated that, for large step sizes, the NSFD structure yields more accurate results than the alternative method. As fellowships, we design the NSFD numerical scheme for the suggested model (1).

Structure of NSFD scheme

On behalf of system (1), we indicate S_m, E_m, I_m, Q_m and R_m as the numerical estimation of $S(t), E(t), I(t), Q(t)$ and $R(t)$ at $= m \Psi$. Anywhere $m = 0, 1, 2, 3, \dots$ and the discretization time step is denoted by Ψ .

$$\begin{aligned} \frac{S_{m+1} - S_m}{\Psi} &= \rho - \tau_1 S_{m+1} I_m - \tau_2 S_{m+1} E_m - \omega S_{m+1} \\ \frac{E_{m+1} - E_m}{\Psi} &= \tau_1 S_m I_m + \tau_2 S_m E_{m+1} - (v_1 + \omega + \Lambda + \varphi) E_{m+1} \\ \frac{I_{m+1} - I_m}{\Psi} &= \Lambda E_m - \theta_1 I_{m+1} - c I_{m+1} \\ \frac{Q_{m+1} - Q_m}{\Psi} &= \varphi E_{m+1} - (\delta + \omega + \theta_2) Q_{m+1} \\ \frac{R_{m+1} - R_m}{\Psi} &= \varphi E_m + c I_m + \delta Q_m - \omega R_{m+1}. \end{aligned} \tag{3}$$

We make the assumption that $S_0 \geq 0, E_0, I_0, Q_0$, and $R_0 \geq 0$. are the beginning values of the discontinuous NSFD SEIQR model (3), which are also non-negative. The discrete NSFD scheme (3) can be derived in its formal version as

$$\begin{aligned} S_{m+1} &= \frac{S_m + \Psi \rho}{1 + \Psi(\tau_1 S_{m+1} I_m + \tau_2 S_{m+1} E_m - \omega)} \\ E_{m+1} &= \frac{E_m + \Psi \tau_1 S_m I_m}{(1 - \Psi(\tau_2 S_m + v_1 + \Lambda + \varphi))} \\ I_{m+1} &= \frac{I_m + \Psi(\Lambda E_m)}{(1 + \Psi(\theta_1 + c))} \\ Q_{m+1} &= \frac{Q_m + \Psi(\varphi E_{m+1})}{(1 + \delta + \omega + \theta_2)} \\ R_{m+1} &= \frac{R_m + \Psi[\varphi E_m + c I + \delta Q]}{(1 + \Psi \omega)}. \end{aligned} \tag{4}$$

Positivity and boundedness of NSFD scheme

For the distinct structure (4), we can define a feasible region similarly to the continuously model (1). NSFD Schemes can preserve the non-negativity of solutions, ensuring that the numerical solution remain bounded such as

$$N_m = S_m + E_m + I_m + Q_m + R_m.$$

Then equations that results from adding each of the five of the equations in (3)

$$\frac{N_{m+1} - N_m}{\Psi} = \rho - \omega N_{m+1} \iff (1 + \Psi\omega) N_{m+1} = \Psi\rho + N_m$$

And

$$N_{m+1} \leq \frac{\Psi\rho}{1 + \Psi\omega} + \frac{N_m}{1 + \Psi\omega} \iff \Psi\omega \sum_{k=1}^m \left(\frac{1}{1 + \Psi\omega}\right)^k + N_0 \left(\frac{1}{1 + \Psi\omega}\right)^m$$

Using the discrete form of Grönwall inequality that is discrete³³⁻³⁵, if $0 < N(0) < \frac{\rho}{\omega}$, then

$$N_m \leq \frac{\rho}{\omega} \left(1 - \frac{1}{(1 + \Psi\omega)^m}\right) + N(0) \left(\frac{1}{1 + \Psi\omega}\right)^m = \frac{\rho}{\omega} + \left(N(0) - \frac{\rho}{\omega}\right) \left(\frac{1}{1 + \Psi\omega}\right)^m$$

Since $\frac{1}{1 + \Psi\omega} < 1$, so we get $N_m \rightarrow \frac{\rho}{\omega}$ as $m \rightarrow \infty$.

Therefore the feasible region for NSFD scheme (4) become

$$\mathcal{K} = \left\{ (\mathbb{S}, \mathbb{E}, \mathbb{I}, \mathbb{Q}, \mathbb{R}) \in \mathbb{R}_+^5 : 0 \leq \mathbb{S}_m + \mathbb{E}_m + \mathbb{I}_m + \mathbb{Q}_m + \mathbb{R}_m \leq \frac{\rho}{\omega} \right\}. \tag{5}$$

We now determine the conditions under which the DFE points are stable. We first analyze the local stability of the equilibrium points.

Local stability of disease free for NSFD scheme

To clarify the locally asymptotically stability (LAS) of DFE points, we take into

$$\begin{aligned} \mathbb{S}_{m+1} &= \frac{\mathbb{S}_m + \Psi\rho}{1 + \Psi(\tau_1\mathbb{S}_{m+1}\mathbb{I}_m + \tau_2\mathbb{S}_{m+1}\mathbb{E}_m - \omega)} = G_1 \\ \mathbb{E}_{m+1} &= \frac{\mathbb{E}_m + \Psi\tau_1\mathbb{S}_m\mathbb{I}_m}{(1 - \Psi(\tau_2\mathbb{S}_m + v_1 + \Lambda + \varphi))} = G_2 \\ \mathbb{I}_{m+1} &= \frac{\mathbb{I}_m + \Psi(\Lambda\mathbb{E}_m)}{(1 + \Psi(\theta_1 + c))} = G_3 \\ \mathbb{Q}_{m+1} &= \frac{\mathbb{Q}_m + \Psi(\varphi\mathbb{E}_{m+1})}{(1 + \delta + \omega + \theta_2)} = G_4 \\ \mathbb{R}_{m+1} &= \frac{\mathbb{R}_m + \Psi[\varphi\mathbb{E}_m + c\mathbb{I} + \delta\mathbb{Q}]}{(1 + \Psi\omega)} = G_5. \end{aligned}$$

As mentioned in Lemma 1, we drive apply the resulting Schur-Cohn criterion^{36,37} to determine that DFE points are locally asymptotically stable.

Lemma 1 *The solutions of equation $\Gamma^2 - \Gamma\Delta + \mathcal{W} = 0$ satisfy $|\Delta_k| < 1, k = 1, 2$, if and only if the following conditions are fulfilled.*

1. $\mathcal{W} < 1$,
2. $1 + \Gamma + \mathcal{W} > 0$,
3. $1 - \Gamma + \mathcal{W} > 0$,

where \mathcal{W} and Γ respectively denote the determinant and trace of Jacobian matrix.

Theorem 1 *If $R_0 < 1$, then the DFE point E_0 of the discrete NSFD model (3) is locally asymptotically stable for all $\Psi > 0$.*

Proof By replacing G_1, G_2, G_3, G_4 and G_5 in Jacobian matrix and then putting DFE point E_0 , we consider the Jacobian matrix

$$J(\mathbb{S}, \mathbb{E}, \mathbb{I}, \mathbb{Q}, \mathbb{R}) = \begin{pmatrix} \frac{\partial G_1}{\partial \mathbb{S}} & \frac{\partial G_1}{\partial \mathbb{E}} & \frac{\partial G_1}{\partial \mathbb{I}} & \frac{\partial G_1}{\partial \mathbb{Q}} & \frac{\partial G_1}{\partial \mathbb{R}} \\ \frac{\partial G_2}{\partial \mathbb{S}} & \frac{\partial G_2}{\partial \mathbb{E}} & \frac{\partial G_2}{\partial \mathbb{I}} & \frac{\partial G_2}{\partial \mathbb{Q}} & \frac{\partial G_2}{\partial \mathbb{R}} \\ \frac{\partial G_3}{\partial \mathbb{S}} & \frac{\partial G_3}{\partial \mathbb{E}} & \frac{\partial G_3}{\partial \mathbb{I}} & \frac{\partial G_3}{\partial \mathbb{Q}} & \frac{\partial G_3}{\partial \mathbb{R}} \\ \frac{\partial G_4}{\partial \mathbb{S}} & \frac{\partial G_4}{\partial \mathbb{E}} & \frac{\partial G_4}{\partial \mathbb{I}} & \frac{\partial G_4}{\partial \mathbb{Q}} & \frac{\partial G_4}{\partial \mathbb{R}} \\ \frac{\partial G_5}{\partial \mathbb{S}} & \frac{\partial G_5}{\partial \mathbb{E}} & \frac{\partial G_5}{\partial \mathbb{I}} & \frac{\partial G_5}{\partial \mathbb{Q}} & \frac{\partial G_5}{\partial \mathbb{R}} \end{pmatrix}. \tag{6}$$

We first locate all of the derivatives utilised in (6) in the following.

$$\begin{aligned}
 \frac{\partial G_1}{\partial S} &= \frac{1}{1 + \Psi(\tau_1 I_m + \tau_2 E_m + \omega)} \frac{\partial G_1}{\partial E} = \frac{-\omega \tau_2 (S_m + \omega \rho)}{(1 + \Psi(\tau_1 I_m + \tau_2 E_m + \omega))^2} \frac{\partial G_1}{\partial I} \\
 &= \frac{-\omega \tau_1 (S_m + \omega \rho)}{(1 + \Psi(\tau_1 I_m + \tau_2 E_m + \omega))^2} \frac{\partial G_1}{\partial Q} = 0, \quad \frac{\partial G_1}{\partial R} = 0. \\
 \frac{\partial G_2}{\partial S} &= \frac{\Psi \tau_1 I_m - \Psi \tau_2 (E_m + \Psi \tau_1 S_m I_m)}{1 - \Psi(\tau_1 I_m + \tau_2 E_m + \omega)} \\
 \frac{\partial G_2}{\partial E} &= \frac{1}{1 - \Psi(\tau_2 S_m + (V_1 + \omega + \Lambda + \varphi))} \\
 \frac{\partial G_2}{\partial I} &= \frac{\Psi \tau_1 S_m}{1 - \Psi(\tau_2 S_m + (V_1 + \omega + \Lambda + \varphi))} \frac{\partial G_2}{\partial Q} = 0, \quad \frac{\partial G_2}{\partial R} = 0 \quad \frac{\partial G_3}{\partial S} = 0, \\
 \frac{\partial G_3}{\partial E} &= \frac{\psi \Lambda}{1 + \psi(\theta_1 + c)}, \quad \frac{\partial G_3}{\partial I} = \frac{1}{1 + \psi(\theta_1 + c)}, \quad \frac{\partial G_3}{\partial Q} = 0, \\
 \frac{\partial G_3}{\partial R} &= 0 \quad \frac{\partial G_4}{\partial S} = 0, \quad \frac{\partial G_4}{\partial E} = \frac{\psi \varphi}{1 + \delta + \omega + \theta_2}, \quad \frac{\partial G_4}{\partial I} = 0, \quad \frac{\partial G_4}{\partial Q} = \frac{1}{1 + \delta + \omega + \theta_2}, \quad \frac{\partial G_4}{\partial R} = 0 \quad \frac{\partial G_5}{\partial S} = 0, \\
 \frac{\partial G_5}{\partial E} &= \frac{\psi \varphi}{1 + \psi \omega}, \quad \frac{\partial G_5}{\partial I} = \frac{\psi c}{1 + \psi \omega}, \quad \frac{\partial G_5}{\partial Q} = \frac{\psi \delta}{1 + \psi \omega}, \quad \frac{\partial G_5}{\partial R} = \frac{1}{1 + \psi \omega}
 \end{aligned}$$

$$J = \begin{vmatrix} \frac{1}{1 + \Psi(\tau_1 I_m + \tau_2 E_m + \omega)} & \frac{-\omega \tau_2 (S_m + \omega \rho)}{(1 + \Psi(\tau_1 I_m + \tau_2 E_m + \omega))^2} & \frac{-\omega \tau_1 (S_m + \omega \rho)}{(1 + \Psi(\tau_1 I_m + \tau_2 E_m + \omega))^2} & 0 & 0 \\ \frac{\Psi \tau_1 I_m - \Psi \tau_2 (E_m + \Psi \tau_1 S_m I_m)}{1 - \Psi(\tau_1 I_m + \tau_2 E_m + \omega)} & \frac{1}{1 - \Psi(\tau_2 S_m + (V_1 + \omega + \Lambda + \varphi))} & \frac{\Psi \tau_1 S_m}{1 - \Psi(\tau_2 S_m + (V_1 + \omega + \Lambda + \varphi))} & 0 & 0 \\ 0 & \frac{\psi \Lambda}{1 + \psi(\theta_1 + c)} & \frac{1}{1 + \psi(\theta_1 + c)} & 0 & 0 \\ 0 & \frac{\psi \varphi}{1 + \delta + \omega + \theta_2} & 0 & \frac{1}{1 + \delta + \omega + \theta_2} & 0 \\ 0 & \frac{\psi \varphi}{1 + \psi \omega} & \frac{\psi c}{1 + \psi \omega} & \frac{\psi \delta}{1 + \psi \omega} & \frac{1}{1 + \psi \omega} \end{vmatrix} \quad (7)$$

Putting the values of all the derivative in (7) we obtain, and also put the DFE point $E_0 = (\frac{\beta}{\theta}, 0, 0, 0)$ From above, we get

$$J(E^0 - \Delta) = \begin{vmatrix} \frac{1}{1 + \Psi \omega} - \Delta & \frac{-\omega \tau_2 (S_m + \omega \rho)}{(1 + \Psi \omega)^2} & \frac{-\omega \tau_1 (S_m + \omega \rho)}{(1 + \Psi \omega)^2} & 0 & 0 \\ 0 & \frac{1}{1 - \Psi(\tau_2 S_m + (V_1 + \omega + \Lambda + \varphi))} - \Delta & \frac{\Psi \tau_1 S_m}{1 - \Psi(\tau_2 S_m + (V_1 + \omega + \Lambda + \varphi))} & 0 & 0 \\ 0 & \frac{\psi \Lambda}{1 + \psi(\theta_1 + c)} & \frac{1}{1 + \psi(\theta_1 + c)} - \Delta & 0 & 0 \\ 0 & \frac{\psi \varphi}{1 + \delta + \omega + \theta_2} & 0 & \frac{1}{1 + \delta + \omega + \theta_2} - \Delta & 0 \\ 0 & \frac{\psi \varphi}{1 + \psi \omega} & \frac{\psi c}{1 + \psi \omega} & \frac{\psi \delta}{1 + \psi \omega} & \frac{1}{1 + \psi \omega} - \Delta \end{vmatrix}$$

Expanding C_1

$$\frac{1}{1 + \Psi \omega} - \Delta \begin{vmatrix} \frac{1}{1 - \Psi(\tau_2 S_m + (V_1 + \omega + \Lambda + \varphi))} - \Delta & \frac{\Psi \tau_1 S_m}{1 - \Psi(\tau_2 S_m + (V_1 + \omega + \Lambda + \varphi))} & 0 & 0 \\ \frac{\psi \Lambda}{1 + \psi(\theta_1 + c)} & \frac{1}{1 + \psi(\theta_1 + c)} - \Delta & 0 & 0 \\ \frac{\psi \varphi}{1 + \delta + \omega + \theta_2} & 0 & \frac{1}{1 + \delta + \omega + \theta_2} - \Delta & 0 \\ \frac{\psi \varphi}{1 + \psi \omega} & \frac{\psi c}{1 + \psi \omega} & \frac{\psi \delta}{1 + \psi \omega} & \frac{1}{1 + \psi \omega} - \Delta \end{vmatrix} = 0.$$

The above matrix has the following eigenvalues

$$\Delta = \frac{1}{1 + \Psi \omega}$$

Expanding C_4

$$\frac{1}{1 + \psi \omega} - \Delta \begin{vmatrix} \frac{1}{1 - \Psi(\tau_2 S_m + (V_1 + \omega + \Lambda + \varphi))} - \Delta & \frac{\Psi \tau_1 S_m}{1 - \Psi(\tau_2 S_m + (V_1 + \omega + \Lambda + \varphi))} & 0 \\ \frac{\psi \Lambda}{1 + \psi(\theta_1 + c)} & \frac{1}{1 + \psi(\theta_1 + c)} - \Delta & 0 \\ \frac{\psi \varphi}{1 + \delta + \omega + \theta_2} & 0 & \frac{1}{1 + \delta + \omega + \theta_2} - \Delta \end{vmatrix} = 0.$$

The above matrix has the following eigenvalues

$$\Delta = \frac{1}{1 + \psi \omega}$$

Expanding C_3

$$\frac{1}{1 + \delta + \omega + \theta_2} - \Delta \begin{vmatrix} \frac{1}{1 - \Psi(\tau_2 S_m + (V_1 + \omega + \Lambda + \varphi))} - \Delta & \frac{\Psi \tau_1 S_m}{1 - \Psi(\tau_2 S_m + (V_1 + \omega + \Lambda + \varphi))} \\ \frac{\psi \Lambda}{1 + \psi(\theta_1 + c)} & \frac{1}{1 + \psi(\theta_1 + c)} - \Delta \end{vmatrix} = 0$$

The above matrix has the following eigenvalues

$$\Delta = \frac{1}{1 + \delta + \omega + \theta_2}$$

To determine the two eigenvalues that are left. From the previous equation, the quadratic equation below is simply derived.

$$\left| \frac{1}{1 - \Psi(\tau_2 S_m + (V_1 + \omega + \Lambda + \varphi))} - \Delta \frac{\Psi \tau_1 S_m}{1 - \Psi(\tau_2 S_m + (V_1 + \omega + \Lambda + \varphi))} \right| = 0.$$

The below quadratic equation can easily be obtained from above equation

$$\Delta^2 - \Delta \left(\frac{1}{1 - \Psi(\tau_2 S_m + (V_1 + \omega + \Lambda + \varphi))} + \frac{1}{1 + \psi(\theta_1 + c)} \right) + \frac{\Psi \tau_1 S_m}{1 - \Psi(\tau_2 S_m + (V_1 + \omega + \Lambda + \varphi))} - \frac{1}{1 - \Psi(\tau_2 S_m + (V_1 + \omega + \Lambda + \varphi))} = 0 \tag{8}$$

Comparing Eq. (8) with $\Delta^2 - \Delta T + D = 0$, we get $T = \left(\frac{1}{1 - \Psi(\tau_2 S_m + (V_1 + \omega + \Lambda + \varphi))} + \frac{1}{1 + \psi(\theta_1 + c)} \right)$ and $D = \frac{\Psi \tau_1 S_m}{1 - \Psi(\tau_2 S_m + (V_1 + \omega + \Lambda + \varphi))} - \frac{1}{1 - \Psi(\tau_2 S_m + (V_1 + \omega + \Lambda + \varphi))}$. If $R_0 < 1$, then all the three condition of lemma 1 remain fulfilled.

1. $D = \frac{\Psi \tau_1 S_m}{1 - \Psi(\tau_2 S_m + (V_1 + \omega + \Lambda + \varphi))} - \frac{1}{1 - \Psi(\tau_2 S_m + (V_1 + \omega + \Lambda + \varphi))} < 1.$
2. $1 + T + D = 1 + \frac{\Psi \tau_1 S_m}{1 - \Psi(\tau_2 S_m + (V_1 + \omega + \Lambda + \varphi))} - \frac{1}{1 - \Psi(\tau_2 S_m + (V_1 + \omega + \Lambda + \varphi))} + \frac{1}{1 - \Psi(\tau_2 S_m + (V_1 + \omega + \Lambda + \varphi))} + \frac{1}{1 + \psi(\theta_1 + c)} > 0.$
3. $1 - T + D = 1 - \frac{\Psi \tau_1 S_m}{1 - \Psi(\tau_2 S_m + (V_1 + \omega + \Lambda + \varphi))} - \frac{1}{1 - \Psi(\tau_2 S_m + (V_1 + \omega + \Lambda + \varphi))} + \frac{1}{1 - \Psi(\tau_2 S_m + (V_1 + \omega + \Lambda + \varphi))} + \frac{1}{1 + \psi(\theta_1 + c)} > 0.$

Therefore, whenever $R_0 < 1$, entirely of the desires for the Schur-Cohn criteria [] covered in Lemma 1 remain fulfilled. Consequently, given that $R_0 < 1$, the discrete NSFD scheme (1)'s DFE point E_0 is LAS. The Fig. 2 illustrates the dynamic behavior of the system, showcasing the intricate relationship between the variable. This physical interpretation of the Fig. 2 offers valuable insights into the system behavior allowing for a deeper understanding of the underlying mechanisms and their implications.

The mathematical imitations displayed in Fig. 2a–c additionally display that the discrete NSFD scheme is unconditionally convergent for model (1) if $R_0 \leq 1$; conversely, if $R_0 \geq 1$ then the answers of NSFD structure (3) diverges to the DEE point for any step size; further demonstrating the unqualified divergence of the discrete NSFD scheme in Fig. 2d.

Theorem 2 The EE point E^* of NSFD system (4.6) is LAS, if $R_0 > 1$.

Proof Let us we take the Jacobian matrix from the above theorem.

In order to determine the eigenvalues of the given matrix, we take the derivative of the matrix and insert additional points.

$$|J_{E^*} - \Delta| = \begin{vmatrix} \frac{1}{1 + \Psi(\tau_1 I_m^* + \tau_2 E_m^* + \omega)} - \Delta & \frac{-\omega \tau_2 (S_m^* + \omega \rho)}{(1 + \Psi(\tau_1 I_m^* + \tau_2 E_m^* + \omega))^2} & \frac{-\omega \tau_1 (S_m^* + \omega \rho)}{(1 + \Psi(\tau_1 I_m^* + \tau_2 E_m^* + \omega))^2} & 0 & 0 \\ \frac{\Psi \tau_1 I_m^* - \Psi \tau_2 (E_m^* + \Psi \tau_1 I_m^* S_m^*)}{1 - \Psi(\tau_1 I_m^* + \tau_2 E_m^* + \omega)} & \frac{1}{1 - \Psi(\tau_2 S_m + (V_1 + \omega + \Lambda + \varphi))} - \Delta & \frac{\Psi \tau_1 S_m}{1 - \Psi(\tau_2 S_m + (V_1 + \omega + \Lambda + \varphi))} & 0 & 0 \\ 0 & \frac{\psi \Lambda}{1 + \psi(\theta_1 + c)} & \frac{1}{1 + \psi(\theta_1 + c)} - \Delta & 0 & 0 \\ 0 & \frac{\psi \varphi}{1 + \delta + \omega + \theta_2} & 0 & \frac{1}{1 + \delta + \omega + \theta_2} - \Delta & 0 \\ 0 & \frac{\psi c}{1 + \psi \omega} & \frac{\psi c}{1 + \psi \omega} & \frac{\psi c}{1 + \psi \omega} & \frac{1}{1 + \psi \omega} - \Delta \end{vmatrix}.$$

Let us we consider the values

$$|J_{E^*} - \Delta| = \begin{vmatrix} k^1 - \Delta & k^2 & k^3 & 0 & 0 \\ k^4 & k^5 - \Delta & k^6 & 0 & 0 \\ 0 & k^7 & k^8 - \Delta & 0 & 0 \\ 0 & k^9 & 0 & k^{10} - \Delta & 0 \\ 0 & k^{11} & k^{12} & k^{13} & k^{14} - \Delta \end{vmatrix}. \tag{9}$$

Here, $k^{14} = \frac{1}{1 + \psi \omega}, k^{10} = \frac{1}{1 + \delta + \omega + \theta_2}, \Delta = k^{14}, \Delta = k^{10}$ and remaining are given by solving the matrix (9)

$$(k^1 - \Delta) \begin{vmatrix} k^5 - \Delta & k^6 \\ k^7 & k^8 - \Delta \end{vmatrix} - k^4 \begin{vmatrix} k^2 & k^3 \\ k^7 & k^8 - \Delta \end{vmatrix} = 0. \tag{10}$$

To solving the above matrix to get the characteristic eq

$$[\Delta^3 + U_3 \Delta^2 + U_2 \Delta + U_1] = 0.$$

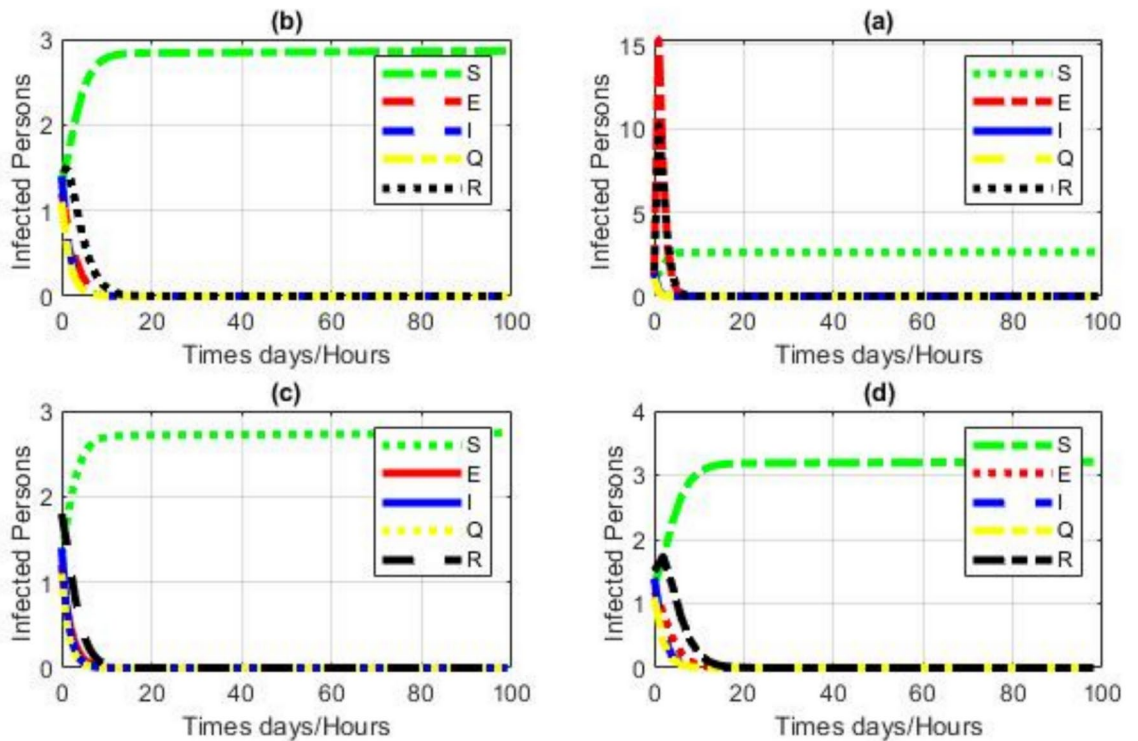


Fig. 2. Numerical simulation of SEIQR model (1) by using NSFD scheme with (a) $\Psi = 0.1$, (b) $\Psi = 0.5$, (c) $\Psi = 1$, (d) $\Psi = 2.5$ other parameters remain fixed as Table 1.

Parameter	Interpretations	Values
ρ	Acquisition rate or birth rates	0.5000
τ_1	Rate at which vulnerable persons are transferred to an infected class	1.05
τ_2	Rate at which vulnerable individuals are transferred to the exposed group	0.005
v_1	Rate at which exposed persons are moved into the quarantine class	0.001
Λ	Rate at which exposed persons are transferred to an infection class	0.085432
φ	Rate at which exposed persons are transferred to the restored class	0.00398
θ_1	Human infection death rate as a result of COVID-19	0.0047876
c	The rate at which diseased people are transitioned into the healed class	0.09871
δ	Rate at which individuals in quarantine migrate to the recovered class	1.05
θ_2	Human mortality in quarantine owing to COVID-19	0.000001231
ω	Rate for human death for each class	0.5000

Table 1. The values and description of the related parameters²⁴.

This revenue;

$$U_3 = (k^1 + k^5 + k^8) > 0.$$

$$U_2 = k^2k^4 + k^1k^5 + k^1k^8 + k^5k^8 + k^6k^7 > 0.$$

$$U_1 = k^1k^5k^8 + k^1k^6k^7 + k^2k^4k^8 - k^3k^4k^7 > 0.$$

$$U_1U_2 - U_3 = (k^1k^5k^8 + k^1k^6k^7 + k^2k^4k^8 - k^3k^4k^7) (k^2k^4 + k^1k^5 + k^1k^8 + k^5k^8 + k^6k^7) - (k^1 + k^5 + k^8) > 0.$$

Altogether the principles are confident, this is arithmetically verified, we dismiss thus states that $U_1, U_2, U_3 > 0$.

Thus the Routh- Hurwitz Criterion³⁸ is fulfilled. So DEE point E^* of NSFD structure (4.6) is LAS, if $R_0 > 1$. Since all of the numbers are positive and can be demonstrated mathematically, we may state that $U_1, U_2, U_3 > 0$. Consequently, the Routh-Hurwitz Criterion³⁸ is met. Therefore, if $R_0 > 1$. DEE point E^* of the NSFD system (4.6) is LAS.

Global stability of equilibria

To find the global stability of DFE and DEE points for NSFD scheme (4), we describe the function $N(y) \geq 0$ such that $K(y) = T - \ln T$ and so $\ln T \leq T - 1$.

The function $\epsilon(y) \geq 0$, such that $K(y) = T - \ln T$ and hence $\ln T \leq T - 1$, is described in order to determine the global stability of DFE and DEE points for NSFD scheme (4).

Theorem 3 For all $\Psi > 0$, the DFE point is globally asymptotically stable (GAS) for NSFD model (4) whenever $\mathcal{R}_0 < 1$.

Proof Create a discrete Lyapunov Function.

$$Y_m(S_m, E_m, I_m, Q_m, R_m) = S^0 N\left(\frac{S_m}{S^0}\right) + \varphi_1 E_m + \varphi_2 I_m + \varphi_3 Q_m + \varphi_4 R_m.$$

where $\varphi_k > 0$ meant for entirely $k = 1, 2, 3, 4, 5$. Therefore, $Y_m > 0$ meant for entirely $S(0) > 0, E(0) > 0, I(0) > 0, Q(0) > 0$ and $R(0) > 0$. In adding, $Y_m = 0$, if and only if $S_m = S^0, E_m = E^0, I_m = I^0, Q_m = Q^0$ and $R_m = R^0$. We take

$$\Delta Y_m = Y_{m+1} - Y_m$$

$$\begin{aligned} \Delta Y_m &= S^0 F\left(\frac{S_{m+1}}{S^0}\right) + \varphi_1 E_{m+1} + \varphi_2 I_{m+1} + \varphi_3 Q_{m+1} + \varphi_4 R_{m+1} - \left(S^0 N\left(\frac{S_m}{S^0}\right) + \varphi_1 E_m + \varphi_2 I_m + \varphi_3 Q_m + \varphi_4 R_m\right). \\ &= S^0 \left(\frac{S_{m+1}}{S^0} - \frac{S_m}{S^0} + \ln \frac{S_m}{S_{m+1}}\right) + \varphi_1 (E_{m+1} - E_m) + \varphi_2 (I_{m+1} - I_m) + \varphi_3 (Q_{m+1} - Q_m) + \varphi_4 (R_{m+1} - R_m). \end{aligned}$$

Expanding the inequity $\ln T \leq T - 1$ above equation become

$$\begin{aligned} \Delta Y_m &\leq S_{m+1} - S_m + S^0 \left(-1 + \frac{S_m}{S_{m+1}}\right) \\ &\quad + \left(-1 + \frac{E_m}{E_{m+1}}\right) \varphi_1 (E_{m+1} - E_m) + \left(-1 + \frac{I_m}{I_{m+1}}\right) \varphi_2 (I_{m+1} - I_m) \\ &\quad + \left(-1 + \frac{Q_m}{Q_{m+1}}\right) \varphi_3 (Q_{m+1} - Q_m) + \left(-1 + \frac{R_m}{R_{m+1}}\right) \varphi_4 (R_{m+1} - R_m). \\ &= -\left(1 - \frac{S^0}{S_{m+1}}\right) (S_{m+1} - S_n) \\ &\quad - \left(1 - \frac{E_m}{E_{m+1}}\right) \varphi_1 (E_{m+1} - E_m) - \left(1 - \frac{I_m}{I_{m+1}}\right) \varphi_2 (I_{m+1} - I_m) \\ &\quad - \left(1 - \frac{Q_m}{Q_{m+1}}\right) \varphi_3 (Q_{m+1} - Q_m) - \left(1 - \frac{R_m}{R_{m+1}}\right) \varphi_4 (R_{m+1} - R_m). \end{aligned}$$

Using system (3), above eq. can be expressed as

$$\begin{aligned} \Delta Y_m &\leq -\left(1 - \frac{S^0}{S_{m+1}}\right) (\rho - \tau_1 S_{m+1} I_m - \tau_2 S_{m+1} E_m - \omega S_{m+1}) \\ &\quad + \left(1 - \frac{E_m}{E_{m+1}}\right) (\varphi_1 \tau_1 S_m I_m + \tau_2 S_m E_{m+1} - (v_1 + \omega + \Lambda + \varphi)) E_{m+1} + \left(1 - \frac{I_m}{I_{m+1}}\right) \varphi_2 (\Lambda E_m - \theta_1 I_{m+1} - c I_{m+1}) \\ &\quad + \left(1 - \frac{Q_m}{Q_{m+1}}\right) \varphi_3 (\varphi E_{m+1} - (\delta + \omega + \theta_2) Q_{m+1}) + \left(1 - \frac{R_m}{R_{m+1}}\right) \varphi_4 (\varphi E_m + c I_m + \delta Q_m - \omega R_{m+1}). \end{aligned}$$

Let $\varphi_k > 0$ for all $k = 1, 2, 3, 4$ be nominated so that.

$$\begin{aligned} (\rho - \tau_1 S_{m+1} I_m - \tau_2 S_{m+1} E_m - \omega S_{m+1}) &= (\varphi_1 \tau_1 S_m I_m + \tau_2 S_m E_{m+1} - (v_1 + \omega + \Lambda + \varphi)) E_{m+1} \\ \varphi_2 (\Lambda E_m - \theta_1 I_{m+1} - c I_{m+1}) &= \varphi_3 (\varphi E_{m+1} - (\delta + \omega + \theta_2) Q_{m+1}) \\ (\varphi E_{m+1} - (\delta + \omega + \theta_2) Q_{m+1}) &= \varphi_4 (\varphi E_m + c I_m + \delta Q_m - \omega R_{m+1}). \end{aligned}$$

Putting the above values, from above eq. we get

$$\begin{aligned} \Delta Y_m \leq & - \left(\left(1 - \frac{S^0}{S_{m+1}} \right) (\rho - \tau_1 S_{m+1} I_m - \tau_2 S_{m+1} E_m - \omega S_{m+1}) \right. \\ & + \left(1 - \frac{E_m}{E_{m+1}} \right) (\varphi_1 \tau_1 S_m I_m + \tau_2 S_m E_{m+1} - (v_1 + \omega + \Lambda + \varphi)) E_{m+1} \\ & + \left(1 - \frac{I_m}{I_{m+1}} \right) \varphi_2 (\Lambda E_m - \theta_1 I_{m+1} - c I_{m+1} + \left(1 - \frac{Q_m}{Q_{m+1}} \right) \varphi_3 (\varphi E_{m+1} - (\delta + \omega + \theta_2) Q_{m+1}) \\ & \left. + \left(1 - \frac{R_m}{R_{m+1}} \right) \varphi_4 (\varphi E_m + c I_m + \delta Q_m - \omega R_{m+1}) \right). \end{aligned}$$

Simple calculation yields

$$\begin{aligned} \Delta Y_m \leq & - \left(\left(1 - \frac{S^0}{S_{m+1}} \right) \left(\rho - \left(1 - \frac{I^0}{I_{m+1}} \right) \varphi_1 (v_1 + \omega + \Lambda + \varphi) \right) E_{m+1} \right. \\ & \left. + \left(1 - \frac{E_m}{E_{m+1}} \right) \varphi_2 \tau_2 S_m E_{m+1} - \left(1 - \frac{Q_m}{Q_{m+1}} \right) \varphi_3 (\delta + \omega + \theta_2) Q_{m+1} + \left(1 - \frac{R_m}{R_{m+1}} \right) \varphi_4 \delta Q_m \right). \end{aligned}$$

As $S^0 = \frac{\rho}{\omega}$ which implies that $S^0 \omega = \rho$. By Substituting ρ in above, we get

$$\begin{aligned} \Delta Y_m \leq & - \left(1 - \frac{S^0}{S_{m+1}} \right) \left(S^0 \omega - \omega S_{m+1} - \left(1 - \frac{I^0}{I_{m+1}} \right) \varphi_1 (v_1 + \omega + \Lambda + \varphi) E_{m+1} \right. \\ & \left. + \left(1 - \frac{E_m}{E_{m+1}} \right) \varphi_2 \rho S_m - \left(1 - \frac{Q_m}{Q_{m+1}} \right) \varphi_3 (\delta + \omega + \theta_2) Q_{m+1} + \left(1 - \frac{R_m}{R_{m+1}} \right) \varphi_4 \delta Q_m \right) \\ & = \frac{-\omega}{S_{m+1}} (S_{m+1} - S^0)^2 - \left(1 - \frac{I^0}{I_{m+1}} \right) \varphi_1 (v_1 + \omega + \Lambda + \varphi) E_m \\ & \quad + \varphi_2 \frac{\rho[\tau_1 \Lambda + \tau_2 (c + \omega + \theta_1)]}{(c + \omega + \theta_1)(v_1 + \varphi + \Lambda + \omega)} - \varphi_3 (\delta + \omega + \theta_2) Q_{m+1} + \varphi_4 \delta Q_m. \end{aligned}$$

Let $H_1 = \frac{\rho[\tau_1 \Lambda + \tau_2 (c + \omega + \theta_1)]}{(c + \omega + \theta_1)(v_1 + \varphi + \Lambda + \omega)}$

$$\begin{aligned} & = \frac{-\omega}{S_{m+1}} (S_{m+1} - S^0)^2 - \left(1 - \frac{I^0}{I_{m+1}} \right) \varphi_1 (v_1 + \omega + \Lambda + \varphi) E_m \\ & \quad + \varphi_2 H_1 R_0 - \varphi_3 (\delta + \omega + \theta_2) Q_{m+1} + \varphi_4 \delta Q_m. \end{aligned}$$

The Fig. 3 illustrate the dynamic behavior of the system, showcasing the intricate relationship between the variable. This physical interpretation of the Fig. 3 offers valuable insights into the system behavior allowing for a deeper understanding of the underlying mechanisms and their implications.

Hence, if $R_0 \leq 1$ then from (above), we can write $\Delta Y_m \leq 0$ on behalf of entirely $m \geq 0$. Subsequently, Y_m is a non-increasing arrangement. Consequently, around occurs a persistent Y such that $\lim_{n \rightarrow \infty} Y_m = Y$ which implies that $\lim_{n \rightarrow \infty} (Y_{m+1} - Y_n) = 0$. Since structure (3) and $\lim_{n \rightarrow \infty} \Delta Y_m = 0$ we have $\lim_{n \rightarrow \infty} S_{m+1} = S^0$ and $\lim_{n \rightarrow \infty} (R_0 - 1)R_n = 0$. For the case $R_0 < 1$, we have $\lim_{n \rightarrow \infty} S_{m+1} = S^0$ and $\lim_{n \rightarrow \infty} E_m = 0, \lim_{n \rightarrow \infty} I_m = 0$. From system (3), we obtain $\lim_{n \rightarrow \infty} E_m = 0, \lim_{n \rightarrow \infty} I_m = 0$ and $\lim_{n \rightarrow \infty} Q_m = 0$. On behalf of the situation $R_0 \leq 1$, we must $\lim_{n \rightarrow \infty} S_{m+1} = S^0$. Consequently, since structure (3), we gain $\lim_{n \rightarrow \infty} R_m = 0, \lim_{n \rightarrow \infty} Q_m = 0, \lim_{n \rightarrow \infty} E_m = 0$, and $\lim_{n \rightarrow \infty} I_n = 0$. Therefore, E_0 is (GAS) globally asymptotically stable.

Theorem 4 For all $\Psi > 0$, the DEE point is globally asymptotically stable (GAS) for NSFD model (4) whenever $R_0 > 1$.

Proof Let us define

$$Y_m(S_m, E_m, I_m, Q_m, R_m) = S^* N \left(\frac{S_m}{S^*} \right) + \varphi_1 E^* N \left(\frac{E_m}{E^*} \right) + \varphi_2 I^* N \left(\frac{I_m}{I^*} \right) + \varphi_3 Q^* N \left(\frac{Q_m}{Q^*} \right) + \varphi_4 R^* N \left(\frac{R_m}{R^*} \right)$$

where $\varphi_i > 0, i = 1, 2, 3, 4, 5$. Which we use later . it is clear that $Y_m(S_m, E_m, I_m, Q_m, R_m) > 0$ for all $S_m > 0, E_m > 0, I_m > 0, Q_m > 0, R_m > 0$. and $Y_m(S^*, E^*, I^*, Q^*, R^*) = 0$.

$$\Delta Y_m = Y_{m+1} - Y_m.$$

So,

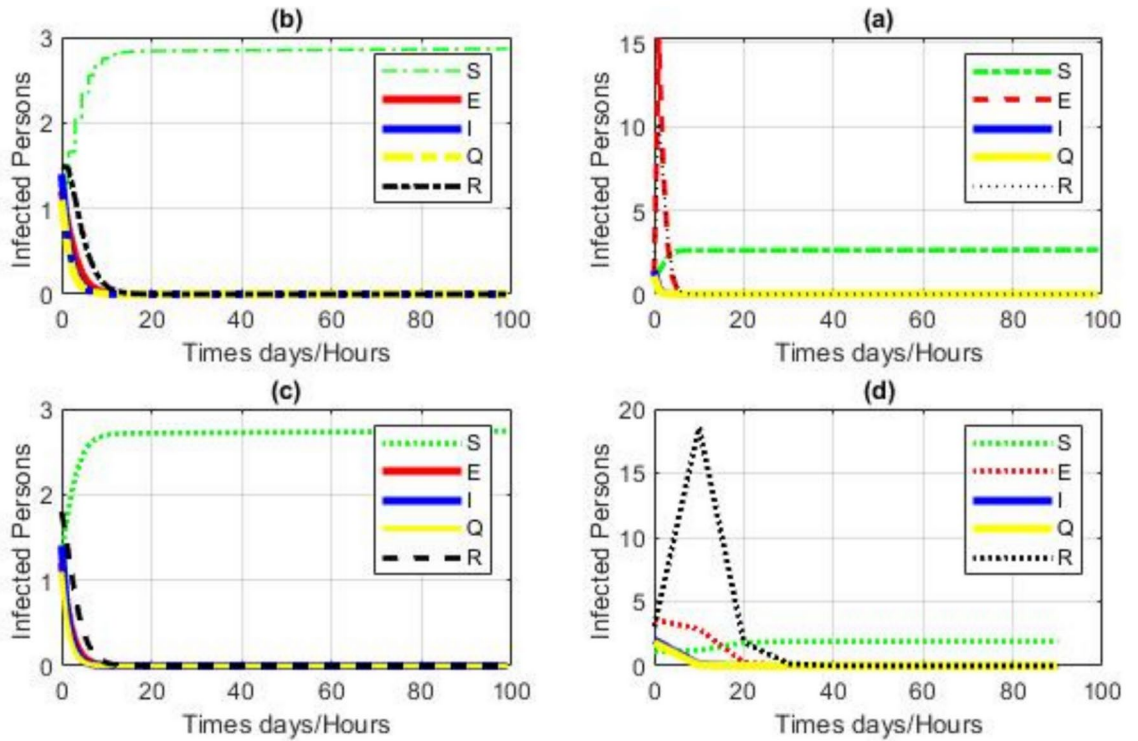


Fig. 3. Numerical simulation for model (1) by using NSFD scheme with (a) $\Psi = 0.1$, (b) $\Psi = 1$, (c) $\Psi = 10$, (d) $\Psi = 30$. (a-c) Stable DFE point with $\tau_1 = 0.005$ (d) Unstable DFE point $\tau_2 = 1.05$ Other parameters stay stable as Table 1.

$$\begin{aligned}
 \Delta Y_m = & \left(S^* N \left(\frac{S_{m+1}}{S^*} \right) + \varnothing_1 E^* N \left(\frac{E_{m+1}}{E^*} \right) \right. \\
 & + \varnothing_2 I^* N \left(\frac{I_{m+1}}{I^*} \right) + \varnothing_3 Q^* N \left(\frac{Q_{m+1}}{Q^*} \right) + \varnothing_4 R^* N \left(\frac{R_{m+1}}{R^*} \right) \Big) \\
 & - \left(S^* N \left(\frac{S_m}{S^*} \right) + \varnothing_1 E^* N \left(\frac{E_m}{E^*} \right) + \varnothing_2 I^* N \left(\frac{I_m}{I^*} \right) + \varnothing_3 Q^* N \left(\frac{Q_m}{Q^*} \right) + \varnothing_4 R^* N \left(\frac{R_m}{R^*} \right) \right) \\
 & + S^* \left(\frac{S_{m+1}}{S^*} - \frac{S_m}{S^*} + \ln \frac{S_m}{S_{m+1}} \right) + \varnothing_1 E^* \left(\frac{E_{m+1}}{E^*} - \frac{E_m}{E^*} + \ln \frac{E_m}{E_{m+1}} \right) \\
 & + \varnothing_2 I^* \left(\frac{I_{m+1}}{I^*} - \frac{I_m}{I^*} + \ln \frac{I_m}{I_{m+1}} \right) + Q^* \left(\frac{Q_{m+1}}{Q^*} - \frac{Q_m}{Q^*} + \ln \frac{Q_m}{Q_{m+1}} \right) \\
 & + \varnothing_4 R^* \left(\frac{R_{m+1}}{R^*} - \frac{R_m}{R^*} + \ln \frac{R_m}{R_{m+1}} \right). \tag{11}
 \end{aligned}$$

By using the inequality $\ln A \leq A - 1$ Now 12 Equation become

$$\begin{aligned}
 \Delta Y_m \leq & S^* \left(\frac{S_{m+1} - S_m}{S^*} + \frac{S_m}{S_{m+1}} - 1 \right) + \varnothing_1 E^* \left(\frac{E_{m+1} - E_m}{E^*} + \frac{E_m}{E_{m+1}} - 1 \right) \\
 & + \varnothing_2 I^* \left(\frac{I_{m+1} - I_m}{I^*} + \frac{I_m}{I_{m+1}} - 1 \right) + \varnothing_3 Q^* \left(\frac{Q_{m+1} - Q_m}{Q^*} + \frac{Q_m}{Q_{m+1}} - 1 \right) + \varnothing_4 R^* \left(\frac{R_{m+1} - R_m}{R^*} + \frac{R_m}{R_{m+1}} - 1 \right) \\
 = & \left(1 - \frac{S^*}{S_{m+1}} \right) (S_{m+1} - S_m) + \varnothing_1 E^* \left(1 - \frac{E^*}{E_{m+1}} \right) (E_{m+1} - E_m) \\
 & + \varnothing_2 I^* \left(1 - \frac{I^*}{I_{m+1}} \right) (I_{m+1} - I_m) + \varnothing_3 Q^* \left(1 - \frac{Q^*}{Q_{m+1}} \right) (Q_{m+1} - Q_m) \\
 & + \varnothing_4 R^* \left(1 - \frac{R^*}{R_{m+1}} \right) (R_{m+1} - R_m). \tag{12}
 \end{aligned}$$

By applying system (3), 12 become

$$\begin{aligned} \Delta Y_m \leq & \left(1 - \frac{S^*}{S_{m+1}}\right) (\rho - \tau_1 S_{m+1} I_m - \tau_2 S_{m+1} E_m - \omega S_{m+1}) \\ & + \varnothing_1 \left(1 - \frac{E^*}{E_{m+1}}\right) (\tau_1 S_m I_m + \tau_2 S_m E_{m+1} - (v_1 + \omega + \Lambda + \varphi) E_{m+1}) \\ & + \varnothing_2 \left(1 - \frac{I^*}{I_{m+1}}\right) (\Lambda E_m - \theta_1 I_{m+1} - c I_{m+1}) + \varnothing_3 \left(1 - \frac{Q^*}{Q_{m+1}}\right) (\varphi E_{m+1} - (\delta + \omega + \theta_2) Q_{m+1}) \\ & + \varnothing_4 \left(1 - \frac{R^*}{R_{m+1}}\right) (\varphi E_m + c I_m + \delta Q_m - \omega R_{m+1}). \end{aligned}$$

After simplification we get,

$$\begin{aligned} \Delta Y_m \leq & \frac{-\tau_1}{S_{m+1}} (S_{m+1} - S^*)^2 - \varnothing_1 E^* \left(N \left(\frac{S^*}{S_{m+1}}\right)\right) \\ & + N \left(\frac{S_{m+1} R_m E^*}{S^* R^* E_{m+1}}\right) + N \left(\frac{I^* E_{m+1}}{E^* I_{m+1}}\right) + E^* \left(\frac{R^* I_{m+1}}{R_{m+1} I^*}\right) \\ & - \varnothing_2 v_1 E^* \left(N \left(\frac{S^*}{S_{m+1}}\right)\right) + N \left(\frac{S_{m+1} R_m R^*}{S^* I^* R_{m+1}}\right) + E^* \left(\frac{R^* R_{m+1}}{E_{m+1} I^*}\right) \\ & - \varnothing \Lambda_3 E^* \left(N \left(\frac{S^*}{S_{m+1}}\right)\right) + N \left(\frac{S_{m+1} R_m E^*}{S^* R^* E_{m+1}}\right) + N \left(\frac{R^* E_{m+1}}{R^* R_{m+1}}\right). \end{aligned}$$

Hence, Y_m is an increasing sequence and there exist $\lim_{n \rightarrow \infty} Y_m = Y$. Therefore, E^* is (GAS) globally asymptotically stable.

Conclusions

This work discusses and analyses a mathematical model that sheds light on the COVID-19 spread mechanism. It estimates the fundamental reproduction number, a key factor in analyzing the local and global stability of DFE and DEE points. The reproduction rate indicates that COVID-19 is moreover below regulator or getting inferior done period. The NSFD systems are established to evaluate some of the simulation's properties, such as local and global stability of DFE and DEE points, as well as the positivity and boundedness of the solutions. It has been discovered that other schemes, such as Euler and Rk-4, are convergent for small step sizes and divergent for large step sizes. Nonetheless, the NSFD method is created, which yields results on behalf of the uninterrupted ideal that are exact, mathematically and biologically plausible, and unconditionally convergent. The NSFD scheme's local and global stability of DFE and DEE points is established through the application of various criteria and conditions. With the associated continuous model, it is confirmed that the suggested NSFD scheme is very dependable for all time step sizes. Our study is advanced in that it develops and tools a novel Non-Standard Finite Difference (NSFD) scheme to analyse the convergence and stability properties of the integer-order COVID-19 model, which has never been done before. Numerical imitations need remained used to confirm the validity of theoretical results. Future work will, include bifurcation analysis and the development of optimal control strategies to better manage the virus's propagation. And also applying this model to real-world datasets or extending the model to include vaccination strategies.

Data availability

Data will be provided by corresponding author on a reasonable request.

Received: 12 October 2024; Accepted: 7 April 2025

Published online: 17 July 2025

References

1. Soresina, A. et al. Two X-linked agammaglobulinemia patients develop pneumonia as COVID-19 manifestation but recover. *Pediatr. Allergy Immunol.* **31**(5), 565–569 (2020).
2. Liu, C. et al. Research and development on therapeutic agents and vaccines for COVID-19 and related human coronavirus diseases (2020).
3. Bootsma, M. C. & Ferguson, N. M. The effect of public health measures on the 1918 influenza pandemic in US cities. *Proc. Natl. Acad. Sci.* **104**(18), 7588–7593 (2007).
4. Ferguson, N. M. et al. *Report 9: Impact of Non-pharmaceutical Interventions (NPIs) to Reduce COVID19 Mortality and Healthcare Demand*, vol. 16. (Imperial College London, 2020).
5. van Doremalen, N. et al. Surface-aerosol stability and pathogenicity of diverse MERS-CoV strains from 2012–2018. *bioRxiv.* (2021).
6. Xu, R. et al. Saliva: potential diagnostic value and transmission of 2019-nCoV. *Int. J. Oral Sci.* **12**(1), 1–6 (2020).
7. Sun, K. et al. Flexible silver nanowire/carbon fiber felt meta composites with weakly negative permittivity behavior. *Phys. Chem. Chem. Phys.* **22**(9), 5114–5122 (2020).
8. Huang, C. et al. Clinical features of patients infected with 2019 novel coronavirus in Wuhan, China. *Lancet* **395**(10223), 497–506 (2020).
9. Li, Q. et al. Early transmission dynamics in Wuhan, China, of novel coronavirus-infected pneumonia. *N. Engl. J. Med.* **382**, 13 (2020).

10. Rihan, F. A. & Alsakaji, H. J. Dynamics of a stochastic delay differential model for COVID-19 infection with asymptomatic infected and interacting people: Case study in the UAE. *Results Phys.* **28**, 104658 (2021).
11. Rihan, F. A., Alsakaji, H. J. & Rajivganthi, C. Stochastic SIRC epidemic model with time-delay for COVID-19. *Adv. Diff. Equ.* **2020**(1), 1–20 (2020).
12. Teklu, S. W. Impacts of optimal control strategies on the HBV and COVID-19 co-epidemic spreading dynamics. *Sci. Rep.* **14**(1), 5328 (2024).
13. Chen, S., Small, M. & Fu, X. Global stability of epidemic models with imperfect vaccination and quarantine on scale-free networks. *IEEE Trans. Netw. Sci. Eng.* **7**(3), 1583–1596 (2019).
14. Li, F., Meng, X., & Wang, X. Analysis and numerical simulations of a stochastic SEIQR epidemic system with quarantine-adjusted incidence and imperfect vaccination. *Comput. Math. Methods Med.* **2018** (2018).
15. Pei, Y., Liu, S., Gao, S., Li, S. & Li, C. A delayed SEIQR epidemic model with pulse vaccination and the quarantine measure. *Comput. Math. Appl.* **58**(1), 135–145 (2009).
16. Volpert, V., Banerjee, M. & Petrovskii, S. On a quarantine model of coronavirus infection and data analysis. *Math. Model. Nat. Phenomena* **15**, 24 (2020).
17. Acuna-Zegarra, M. A., Diaz-Infanteb, S., Baca-Carrasco, D. & Olmos-Liceaga, D. COVID-19 optimal vaccination policies: a modeling study on efficacy, natural and vaccine-induced immunity responses. *MedRxiv* (2020).
18. Kotola, B. S., Teklu, S. W. & Abebaw, Y. F. Bifurcation and optimal control analysis of HIV/AIDS and COVID-19 co-infection model with numerical simulation. *PLoS ONE* **18**(5), e0284759 (2023).
19. Teklu, S. W. Mathematical analysis of the transmission dynamics of COVID-19 infection in the presence of intervention strategies. *J. Biol. Dyn.* **16**(1), 640–664 (2022).
20. Shah, A., Marks, P. W. & Hahn, S. M. Unwavering regulatory safeguards for COVID-19 vaccines. *JAMA* **324**(10), 931–932 (2020).
21. Michlin-Shapir, V., & Khvostunova, O. The Rise and Fall of Sputnik V. *Institute of Modern Russia*, October. (2021).
22. Escobar, L. E., Molina-Cruz, A. & Barillas-Mury, C. BCG vaccine protection from severe coronavirus disease 2019 (COVID-19). *Proc. Natl. Acad. Sci.* **117**(30), 17720–17726 (2020).
23. Ahmed, A., Salam, B., Mohammad, M., Akgül, A. & Khoshnaw, S. H. Analysis coronavirus disease (COVID-19) model using numerical approaches and logistic model. *Aims Bioengineering* **7**(3), 130–146 (2020).
24. Butt, A. I. K., Ahmad, W., Rafiq, M. & Baleanu, D. Numerical analysis of Atangana-Baleanu fractional model to understand the propagation of a novel corona virus pandemic. *Alex. Eng. J.* **61**(9), 7007–7027 (2022).
25. Sameni, R. Mathematical modeling of epidemic diseases; a case study of the COVID-19 coronavirus. *arXiv preprint arXiv:2003.11371*. (2020).
26. He, J. J. et al. Stability analysis of a nonlinear malaria transmission epidemic model using an effective numerical scheme. *Sci. Rep.* **14**(1), 17413 (2024).
27. Arino, J., & Driessche, P. V. D. The basic reproduction number in a multi-city compartmental epidemic model. In *Positive Systems*, 135–142 (Springer, 2003)
28. Khan, I. U. et al. The stability analysis of a nonlinear mathematical model for typhoid fever disease. *Sci. Rep.* **13**(1), 15284 (2023).
29. Mickens, R. E. Dynamic consistency: a fundamental principle for constructing nonstandard finite difference schemes for differential equations. *J. Differ. Eq. Appl.* **11**(7), 645–653 (2005).
30. A positivity-preserving non standard finite difference scheme for the damped wave equation.
31. Mickens, R. E. & Jordan, P. M. A new positivity-preserving nonstandard finite difference scheme for the DWE. *Numer. Methods Partial Differ. Equ. Int. J.* **21**(5), 976–985 (2005).
32. Dang, Q. A. & Hoang, M. T. Complete global stability of a metapopulation model and its dynamically consistent discrete models. *Qual. Theory Dyn. Syst.* **18**, 461–475 (2019).
33. Pachpatte, B. G. On the discrete generalizations of Gronwall's inequality. *J. Indian Math. Soc* **37**, 147–156 (1973).
34. Clark, D. S. Short proof of a discrete Gronwall inequality. *Discret. Appl. Math.* **16**(3), 279–281 (1987).
35. Dixon, J. & McKee, S. Weakly singular discrete Gronwall inequalities. *ZAMM-J. Appl. Math. Mech./Zeitschrift für Angewandte Mathematik und Mechanik* **66**(11), 535–544 (1986).
36. Khatun, Z., Islam, M. S. & Ghosh, U. Mathematical modeling of hepatitis B virus infection incorporating immune responses. *Sens. Int.* **1**, 100017 (2020).
37. Mulero-Martínez, J. I. Modified Schur-Cohn criterion for stability of delayed systems. *Math. Probl. Eng.* **2015**(1), 846124 (2015).
38. Khan, T., Zaman, G. & Chohan, M. I. The transmission dynamic and optimal control of acute and chronic hepatitis B. *J. Biol. Dyn.* **11**(1), 172–189 (2017).

Acknowledgements

The authors extend their appreciation to Taif University, Saudi Arabia, for supporting this work through project number (TU-DSPP-2024-145).

Author contributions

A. Aljohani: conceptualized the research problem and designed the overall study. Contributed to the development and mathematical formulation of the SEIQR model and provided critical insights into its epidemiological aspects. S. Mustafa: focused on the theoretical analysis of the SEIQR model, including the calculation and evaluation of the fundamental threshold quantity R_0 . Played a central role in validating analytical results through numerical simulations and refining mathematical proofs. S. A. Khan: implemented the numerical simulations and ensured consistency between theoretical and computational results. Evaluated the NSFD scheme's performance and contributed to the visualization and presentation of the results. A. Alhushaybari: reviewed and validated the mathematical modeling, computational approaches, and numerical techniques. Contributed to manuscript drafting and editing, ensuring technical accuracy and clarity. H. Mukalazi (Corresponding Author): coordinated the overall project, guided the interpretation of results in the context of epidemiology, and provided leadership in integrating contributions from all authors. Finalized the manuscript for submission and managed correspondence during the review process.

Funding

This research was funded by Taif University, Saudi Arabia, Project No. (TU-DSPP-2024-145).

Declarations

Competing interests

The authors declare no competing interests.

Additional information

Correspondence and requests for materials should be addressed to H.M.

Reprints and permissions information is available at www.nature.com/reprints.

Publisher's note Springer Nature remains neutral with regard to jurisdictional claims in published maps and institutional affiliations.

Open Access This article is licensed under a Creative Commons Attribution-NonCommercial-NoDerivatives 4.0 International License, which permits any non-commercial use, sharing, distribution and reproduction in any medium or format, as long as you give appropriate credit to the original author(s) and the source, provide a link to the Creative Commons licence, and indicate if you modified the licensed material. You do not have permission under this licence to share adapted material derived from this article or parts of it. The images or other third party material in this article are included in the article's Creative Commons licence, unless indicated otherwise in a credit line to the material. If material is not included in the article's Creative Commons licence and your intended use is not permitted by statutory regulation or exceeds the permitted use, you will need to obtain permission directly from the copyright holder. To view a copy of this licence, visit <http://creativecommons.org/licenses/by-nc-nd/4.0/>.

© The Author(s) 2025